The sensors for the intelligent micro washing system
Sensor array 1

Work report 8, 2-Oct-96
Geert Langereis

1. Introduction **2**

2. Specifications of the electrolyte **4**

2.1 Water hardness 4
2.2 Temperature 4
2.3 Bleach effectiveness 4
2.4 Conductivity 5

3. Design and modelling of the devices **6**

3.1 Conductivity 6
3.2 Working electrode 8
3.3 Temperature 9
3.4 Lay-out of the integrated sensor array 9
3.5 The multipurpose sensor structure 10

4. Interpreting conductivity and temperature **11**

4.1 The effect of temperature 11
4.2 Mathematical treatment 11
4.3 A preliminary measurement 14

5. Eliminating the reference electrode during amperometry **15**

5.1 The reference with chrono amperometry 15
5.2 Amperomtry with an added AC signal 15

6. A stimulus-response measurement **17**

6.1 Precipitation of $CaOH_2$ on a conductivity cell 17
6.2 Lay-out of the devices 19

7. Conclusions **20**

A. The silicon process **22**

B. References **24**

1. Introduction

After concluding that a lot of washing parameters of interest can be measured using planar metal films, the next step is to show it. This first sensor array will be referred to as “Array 1”. Three basic elements were chosen to be implemented:

1. A conductivity cell;
2. A working electrode for amperometric (or potentiometric) measurements and local pH control;
3. A resistor for thermoresistive measurements and heating.

This first realisation of a sensor array during the project is meant to learn about some problems:

1. Getting familiar with these sensors and their use;
2. How do these sensors interfere when simultaneously used;
3. Can the achieved data be combined in order to increase accuracy or to find new parameters. For example, in order to find the ionic strength from the measured conductivity one needs the local temperature;
4. What does an actuator (heating, pH control) do with the response of other sensors. Find a nice stimulus-response measurement which yields new information on the system;
5. During chrono amperometry for determining the bleach efficiency, a (glass) reference electrode is needed. Is it possible to use a miniaturised reference electrode or pseudo reference electrode?
6. Is it possible to integrate the sensor structures into a multipurpose-sensor structure. In a preliminary research of four students such a combined sensor was developed. Less attention has been paid to the optimisation of this multi-sensor. Therefor a new design will be tested;
7. Is it necessary to use an insulated resistor for heating when measuring temperature with a second resistor? During some test measurements, the measuring resistor appeared to pick up directly the applied potential of the heating resistor. The resistive coupling between sensor and actuator might be a problem in future;

Three types of devices will be produced. The first type consists of three separate structures placed on a chip of 1.5×2.3 mm. This type of sensor array will be referred to as the “integrated sensor array”. With this array, experiments will be carried out to investigate questions 1 to 5. The second type is an optimisation of the students’ multipurpose-sensor structure. In order to find an answer to question 7, some pairs of resistors will be developed, either insulated or in contact with the electrolyte.

The methods described in this work report all have the same aim: creating an integrated sensor array. Figure 1.1 shows an overview in terms of sensor terminology.

The environment to be measured was evaluated in a previous work report. It was concluded what parameters are of interest for having a complete as possible idea of the state of a washing process.

These parameters will be measured using basic sensor structures. The physical and chemical properties of these structures enable an operator to extract information from the system. The choice was made to use inert metal structures only. Problem 6, as mentioned above, concerns this part of the sensor.

Basic sensor structures will only yield information when they are controlled by an electronic circuitry in order to set an operational point. Depending on the signals with which the control logic supplies the structures, several types of information can be extracted from the system. A stimulus/response measurement is a typical example of a control logic part. In chapter 4 and 6 of this work report two stimulus response measurements are evaluated. Chapter 5 gives an idea for a smart control logic which can find the desired operational point.

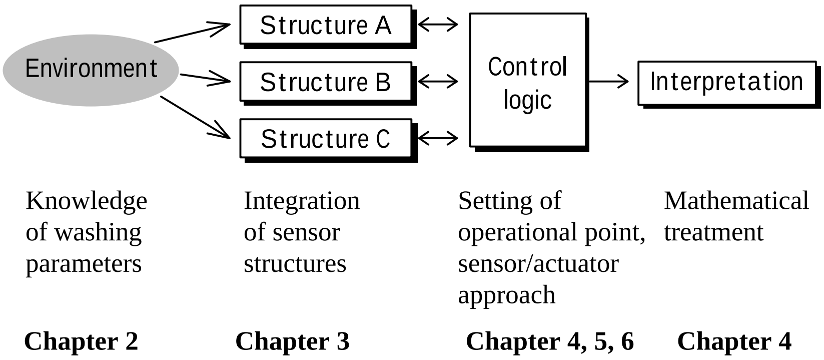

Figure 1.1: Points of interest during array development

When a set of parameters is measured, the interpretation of this information might yield new information or more accurate information. Chapter 4 says something about the interpretation of the measured temperature and conductivity.

2. Specifications of the electrolyte

To design a sensor, it is important to know about the ranges of the parameters to be measured. In washing processes there will be a huge difference between the situation before washing (tap water) and during washing (after applying the detergent).

2.1 Water hardness

Figure 2.1 shows the distribution of the hardness ions in the tap water of 44 Dutch cities in 1986 [1]. The calcium concentration appears to be normally distributed around 1.41 mM (pCa » 2.8).

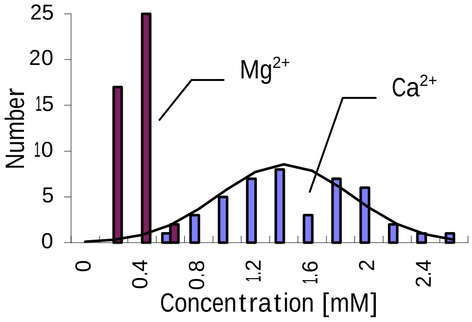

Figure 2.1: Concentration of hardness-ions in Dutch tap water

When the laundry is being soaked by the water, the calcium concentration rises to the magnitude of about 10 mM (pCa » 2). After applying detergent, the concentration of free Ca^{2+} is being reduced to 10^{-4}-10^{-5} M because of the builder effect. Generally using phosphate based builders the pCa becomes 5.6, with zeolite based builders this value is about 4.2.

So for measuring hardness, a calcium sensor is needed which measures for over four decades. For the magnesium concentration the empirical relation $Mg^{2+} : Ca^{2+} = 1 : 4$ can be used during all phases of the washing process.

2.2 Temperature

The temperature of tap water is about 10°C but can be lower (down to 5°C) in winter. During the main wash the water will be heated to either 40, 60 or 90°C.

2.3 Bleach effectiveness

The concentration of bleaching compounds is generally 6 - 8 mM for perborate based systems (hydrogen peroxide) and 1 - 2 mM for peracid based systems.

2.4 Conductivity

The conductivity distribution of Dutch tap water is plotted in the left Figure 2.2. The average is 487 µS/cm with a standard deviation of 157 µS/cm.

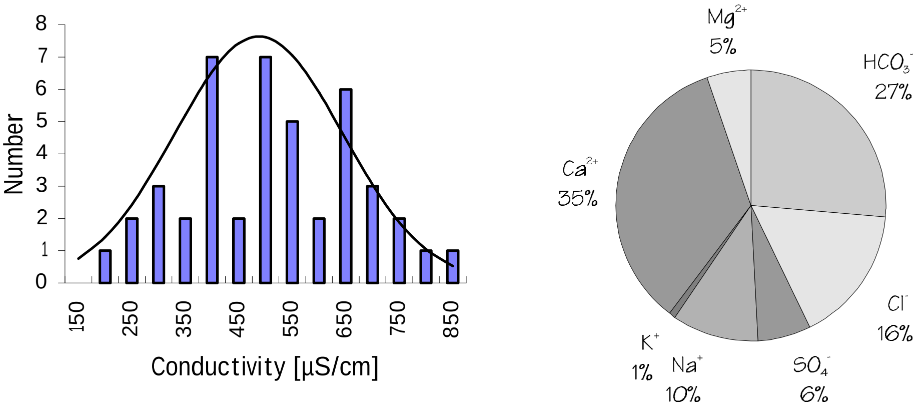

Figure 2.2: Distribution of conductivity in Dutch tap water (left) and the contribution of the separate ions to this conductivity (right)

The ions that contribute to the conductivity can be found in the right figure. It appears that Ca^{2+}, Na^+, Cl^- and HCO_3^- determine the conductivity of tap water for almost 90%.

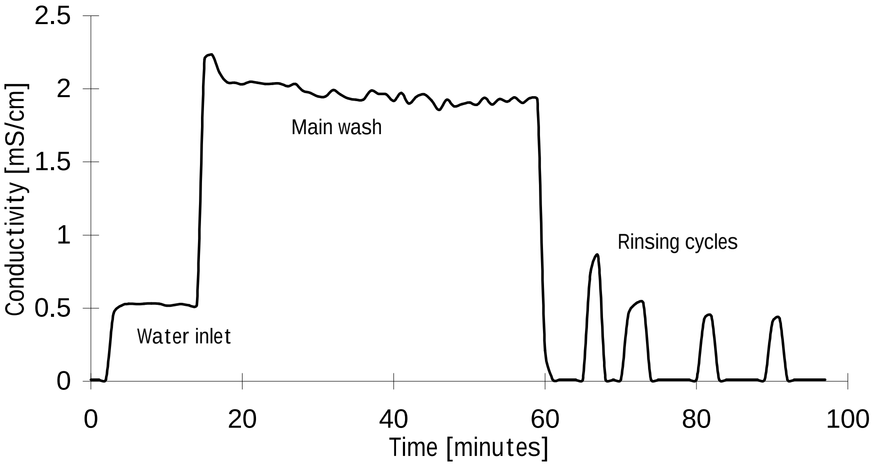

Figure 2.3: Conductivity during washing

During the main wash (Figure 2.3, taken from an internal Unilever data source) the conductivity increases to about 2 mS/cm. So a conductivity sensor needs to cover about 2.5 decades.

3. Design and modelling of the devices

This chapter describes the design of three sensor elements to be implemented in the sensor array.

3.1 Conductivity

The conductivity cell will be an interdigitated finger structure. The model for this element is given in Figure 3.1.

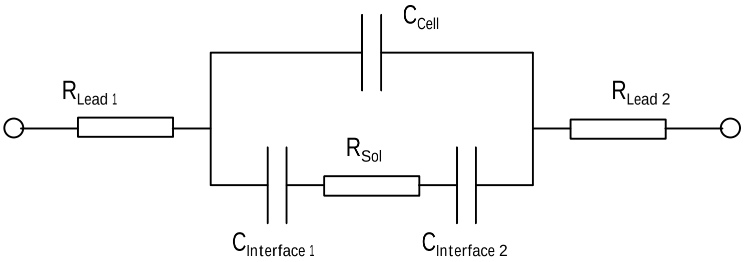

Figure 3.1: Equivalent circuit for finger structure

R_{Sol}:

The solution resistance is the actual component of interest and is related to the conductivity κ_{Sol} by the cell constant K_{Cell}:

$$R_{Sol} = \frac{K_{Cell}}{\kappa_{Sol}} \tag{3.1}$$

The cell constant is for an interdigitated finger structure with N fingers, finger spacing S, finger width W and finger length L equal to [2]:

$$K_{Cell} = \frac{2}{(N-1)L} \cdot \frac{K(k_1)}{K(k_2)} \tag{3.2}$$

with

$$K(k) = \int_0^1 \frac{1}{\sqrt{(1-t^2)(1-k^2t^2)}}\,dt \qquad k_1 = \cos\left(\frac{\pi}{2} \cdot \frac{W}{S+W}\right) \quad k_2 = \cos\left(\frac{\pi}{2} \cdot \frac{S}{S+W}\right)$$

So the cell constant depends entirely on the geometry of the sensor.

R_{Lead}:

The lead resistance is the result of the series resistances of the connecting wires (± 50 cm), the dipstick length and the bonding wires. A value of 1 Ω was measured for both lead 1 and lead 2.

C_{Cell}:

The cell capacitance represents the capacitive coupling between the two electrodes and is equal to:

$$C_{Cell} = \frac{\varepsilon_0 \varepsilon_{Sol}}{K_{Cell}} \tag{3.3}$$

with $e_{Sol} = e_{Water} = 80$.

$C_{Interface}$:

The interface capacitance depends on the electrode material an the electrolyte but can be approximated by:

$$C_{Interface} = A \cdot C_{Char} = W \cdot L \cdot N \cdot C_{Char} \tag{3.4}$$

where A is the electrode surface and C_{Char} the characteristic interface capacitance of the electrode\electrolyte system (C_{Char} = 10-20 µF/cm^2) [3].

Optimisation

The frequencies between which the conductivity can be found from the impedance can be determined from the impedance equation:

$$\begin{aligned} Z(\omega) &= 2R_{Lead} + \frac{x}{j\omega C_{Cell} x + 1} \\ x &= R_{Sol} + \frac{2}{j\omega C_{Interface}} \end{aligned} \tag{3.5}$$

The cut-off frequencies are:

$$f_{lo} = \frac{1}{2\pi\left(R_{Lead} C_{interface} + 2R_{Lead} C_{Cell} + \tfrac{1}{2} R_{Sol} C_{Interface}\right)} \approx \frac{1}{\pi R_{Sol} C_{Interface}} \tag{3.6}$$

$$f_{hi} = \frac{1}{2\pi R_{Sol} \frac{C_{interface} C_{Cell}}{C_{interface} + 2C_{Cell}}} \approx \frac{1}{2\pi R_{Sol} C_{Cell}} \tag{3.7}$$

or in terms of conductivity parameters:

$$f_{lo} = \frac{\kappa_{sol}}{\pi W \cdot L \cdot N \cdot C_{char} K_{Cell}} \tag{3.8}$$

$$f_{hi} = \frac{\kappa_{sol}}{2\pi \varepsilon_0 \varepsilon_{Sol}} \tag{3.9}$$

In order to make the lower boundary frequency (3.8) as low as possible, the geometrical term

$$W \cdot L \cdot N \cdot K_{Cell}(N, L, S, W)$$

should be maximised. When using a square structure of L×L, one variable can be eliminated because:

$$L = N \cdot (W + S) \tag{3.10}$$

Three sets of parameters were chosen as given in Table 3.1.

Table 3.1: Chosen parameters

	Type 1	Type 2	Type 3
S [µm]	15	5	115
W [µm]	100	200	115
L [µm]	1035	1025	1155
N	9	5	5
C_{Cell} [pF]	5.29	3.48	1.64
R_{Sol} [kΩ] *	2.68	4.08	8.66
R_{Lead} [Ω]	1	1	1
$C_{Interface}$ [nF]	13.04	14.36	9.30
K_{Cell} [m^{-1}]	134	204	433
f_{lo} [kHz] *	9.10	5.50	3.95
f_{hi} [GHz] *	1.12	1.12	1.12

* For κ_{Sol} = 500 µS/cm

The upper limit of the frequency range (3.9) is being determined by the conductivity of the electrolyte.

Result

Between the frequencies f_{lo} and f_{hi} the measured impedance of the system is equal to:

$$Z(\omega) = 2R_{Lead} + R_{Sol} \tag{3.11}$$

with R_{Sol} dependent on the conductivity according to (3.1).

3.2 Working electrode

The primary aim of the working electrode is to measure hydrogen peroxide by using chrono-amperometry. The reaction involved is:

$$H_2O_2 \rightarrow O_2 + 2H^+ + 2e^- \tag{3.12}$$

which occurs at a positive potential step. The current response is given by the Cottrell equation:

$$i(t) = nFAC_O\sqrt{\frac{D_O}{\pi t}} \tag{3.13}$$

with F the Faraday constant, n the number of electrons transferred, A the actuator area, C_O the bulk H_2O_2 concentration and D_O the diffusion coefficient (approximately $1.6 \cdot 10^{-5}$ cm/s at pH<10 [4]).

3.3 Temperature

The resistance of a metal strip is:

$$R_0 = \frac{\rho l}{wh} \tag{3.14}$$

where w the width, h the thickness and l the length of the strip and ρ the specific resistivity of the metal. For platinum, the resistivity at room temperature is $1.0 \cdot 10^{-5}$ Ω·cm. The used structure has an intended thickness of 250 nm, a width of 10 µm and a length of 14 mm. Therefore, the nominal resistance will be 560 Ω.

The change in resistance due to temperature can be written as:

$$R = R_0\left(1 + \alpha\left(T - T_0\right)\right) \tag{3.15}$$

with α the temperature coefficient. This coefficient is 0.00392 °C^{-1} for platinum with a linearity of 0.2% between 0-100 °C [5].

3.4 Lay-out of the integrated sensor array

Table 3.2 shows the final chip lay-outs for the integrated sensor arrays. The squares indicate the areas which are in contact with the electrolyte. Notice that the temperature sensors are insulated from the electrolyte.

Table 3.2: Chip lay-outs for the sensor arrays

Type 1	Type 2	Type 3
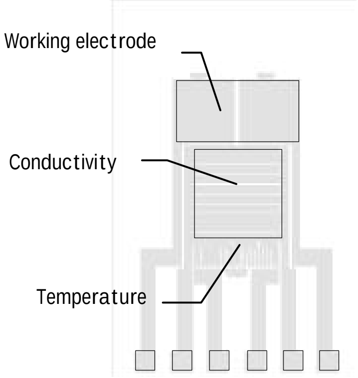	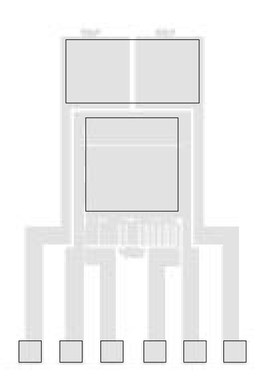	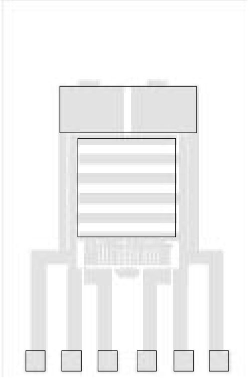
Conductivity		
S = 15 µm	S = 5 µm	S = 115 µm
W = 100 µm	W = 200 µm	W = 115 µm
L = 1035 µm	L = 1025 µm	L = 1155 µm
N = 9	N = 5	N = 5
Temperature		
L = 14 mm	L = 14 mm	L = 14 mm
W = 10 µm	W = 10 µm	W = 10 µm
Working electrode		
A = 2 × 0.50 mm^2	A = 2 × 0.50 mm^2	A = 2 × 0.40 mm^2

3.5 The multipurpose sensor structure

In the previous devices, the distance between the sensors in the array was still about 100 µm. In order to measure several parameters in exactly the same sample, one should measure using the same structure.

During a preliminary research, four students developed an integrated sensor structure which could measure conductivity, temperature and Fe^{2+} concentration [6]. The sensor structure they proposed was based on an interdigitated finger structure. In this structure some gaps were made in order to create a path with a significant resistance for temperature measurements. The whole structure can be used as a working electrode.

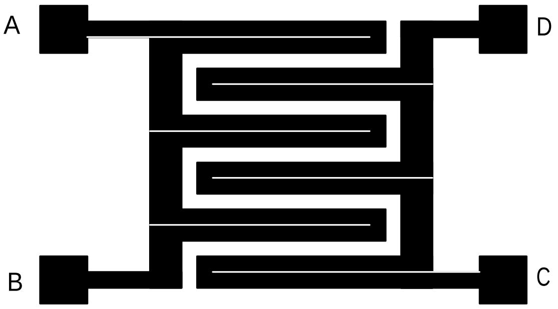

Figure 3.2: Integrated sensor concept

Figure 3.2 shows the idea. Between inputs A-B or C-D a resistive path is present for temperature measurement or heating. When both A-B and C-D are short cutted then the structure can be used as an interdigitated finger cell.

Table 3.3: Chip lay-outs for the integrated sensors

Type A	Type B
Conductivity	
S = 5 µm	S = 15 µm
W = 200 µm	W = 100 µm
L = 1025 µm	L = 1035 µm
N = 5	N = 9
Temperature	
L = 10.25 mm (2×)	L = 8.28 mm (2×)
W = 47 µm	W = 45 µm
Working electrode	
$A = 2 \times 0.48\ mm^2$	$A = 2 \times 0.42\ mm^2$
Active area	
$A = 1.025 \times 1.025\ mm^2$	$A = 1.035 \times 1.035\ mm^2$

The conductivity parts of integrated sensor arrays type 1 and 2 were adapted to form the multipurpose sensors. Table 3.3 shows the chip lay-outs. The resistance of the temperature sensor for type A and B are respectively 87 W and 74 W.

4. Interpreting conductivity and temperature

Measuring conductivity is not interesting unless the measured value is normalised for temperature. The reason for this is that at higher temperature, ions become more mobile and will cause an increase in conductivity. So with the same concentration, an increase in temperature results in an increase in conductivity. In general, the measured conductivity is compensated to 25°C by using a temperature measurement.

4.1 The effect of temperature

The total conductivity of an electrolyte expressed in terms of the limiting molar conductivities of the separate ions can be expressed by:

$$\Lambda = \sum_{i=1}^{I} z_i c_i \lambda_i(T) \tag{4.1}$$

with z_i the charge of ion i, c_i the concentration, I the number of ions and $\lambda_i(T)$ the limiting molar conductivity of ion i. This last one is dependent on temperature. Since a conductivity measurement can not differentiate among different ions, it is not possible to eliminate mathematically the temperature effect.
Industrial temperature compensation methods use the average temperature dependency of L which is about 2%/°C. This linear fit is the most simple approximation of the temperature dependency and is suitable for most pure water applications for a moderate temperature range [7]. More sophisticated fits compensate by using a third order polynomial, but this method is electrolyte and concentration dependent [8].

A more complicated temperature compensation uses a polynomial fit for the limiting molar conductivities of the separate ions [9]. A third order approximation was proposed by Harned and Owen [10] and tabulated for several ions. The equation is

$$\lambda_i(T) = \lambda_i^0 \left[1 + k_{i,1}(T-25) + k_{i,2}(T-25)^2 + k_{i,3}(T-25)^3 \right] \tag{4.2}$$

with λ_i^0 the limiting molar conductivity of ion i at 25°C.

4.2 Mathematical treatment

The generalised polynomial fit of order J with respect to temperature T_0 can be written as:

$$\lambda_i(T) = \lambda_i^0 \sum_{j=0}^{J} k_{i,j} \left(T - T_0 \right)^j \tag{4.3}$$

For N conductivity measurements and I = 2 ions, a matrix equation can be formed using equation (4.1) and (4.3):

$$\begin{bmatrix} \Lambda_1 \\ \Lambda_2 \\ . \\ . \\ \Lambda_N \end{bmatrix} = \begin{bmatrix} 1 & 1 & (T_1 - T_0) & (T_1 - T_0) & (T_1 - T_0)^2 & . & (T_1 - T_0)^J \\ 1 & 1 & (T_2 - T_0) & (T_{21} - T_0) & (T_2 - T_0)^2 & . & . \\ . & . & . & & & & \\ . & . & . & & & & \\ 1 & 1 & . & & & & \end{bmatrix} \cdot \begin{bmatrix} 1 & 0 \\ 0 & 1 \\ k_{1,1} & 0 \\ 0 & k_{2,1} \\ . & . \\ 0 & k_{2,J} \end{bmatrix} \cdot \begin{bmatrix} z_1 c_1 \lambda_1^0 \\ z_2 c_2 \lambda_2^0 \end{bmatrix} \qquad (4.4)$$

or

$$\overline{\Lambda} = \overline{\overline{T}} \cdot \overline{\overline{K}} \cdot \overline{z}$$

The question rises whether it is possible to calculate the vector $\overline{z}$ (containing the concentration information) from known $\overline{\overline{T}}$ and $\overline{\overline{K}}$ matrices and a measured $\overline{\Lambda}$ vector.

Identification of ions by the coefficients matrix K

If equation (4.4) can be solved, the present ions can be identified by comparing the columns of matrix $\overline{\overline{K}}$ to known coefficients. Afterwards, the corresponding concentrations can be found from vector $\overline{z}$.

In order to solve $\overline{\overline{K}} \cdot \overline{z} = \overline{\overline{T}}^{-1} \cdot \overline{\Lambda}$, the matrix $\overline{\overline{T}}$ must be square and have an inverse. The first condition can be met by choosing the number of experiments $N = (J+1) \cdot I$. The second one will never be met because de determinant of $\overline{\overline{T}}$ will always be zero because of the identical columns.

Known coefficients

This problem will not appear when the $\overline{\overline{K}}$ matrix is assumed to be known. Equation (4.4) can be written as

$$\begin{bmatrix} \Lambda_1 \\ \Lambda_2 \\ . \\ . \\ \Lambda_N \end{bmatrix} = \begin{bmatrix} \sum_{j=0}^{J} k_{1,j}(T_1 - T_0)^j & \sum_{j=0}^{J} k_{2,j}(T_1 - T_0)^j & . & \sum_{j=0}^{J} k_{I,j}(T_1 - T_0)^j \\ \sum_{j=0}^{J} k_{1,j}(T_2 - T_0)^j & \sum_{j=0}^{J} k_{2,j}(T_2 - T_0)^j & . & . \\ . & . & . & . \\ \sum_{j=0}^{J} k_{1,j}(T_N - T_0)^j & . & . & \sum_{j=0}^{J} k_{I,j}(T_N - T_0)^j \end{bmatrix} \cdot \begin{bmatrix} z_1 c_1 \lambda_1^0 \\ z_2 c_2 \lambda_2^0 \\ . \\ z_I c_I \lambda_I^0 \end{bmatrix} \qquad (4.5)$$

by calculating the $\overline{\overline{T}} \cdot \overline{\overline{K}}$ matrix. Notice that the determinant of this matrix is generally not equal to zero. The concentrations will follow from

$$\overline{z} = \left(\overline{\overline{T}} \cdot \overline{\overline{K}}\right)^{-1} \cdot \overline{\Lambda} \qquad (4.6)$$

where the number of necessary experiments is now reduced to $N = I$.

Estimation method

The previous method is not very accurate because the number of parameters to be solved is equal to the number of experiments. It is better to do more measurements ($N > I$) and use an estimation method.

In order to find the best fit from the measurements, some theory concerning parameter estimation is necessary.

Consider the generalised system:

$$\overline{\Lambda} = \overline{\overline{B}} \cdot \overline{z} + \overline{v} \tag{4.7}$$

with

$\overline{\Lambda}$ *the vector containing the measurements,*
$\overline{\overline{B}}$ *a matrix representing the system (in our case equal to* $\overline{\overline{T}} \cdot \overline{\overline{K}}$*),*
$\overline{z}$ *the input vector to be estimated and*
$\overline{v}$ *the noise or error in the measurement.*

Assume the conditions:

the elements of $\overline{v}$ *are uncorrelated and have equal standard deviations* s_v*,*
$\overline{z}$ *and* $\overline{v}$ *are uncorrelated and*
the moment matrix of $\overline{z}$ *satisfies* $\overline{\overline{C}}_{\overline{z}} \rightarrow \infty$.

The linear minimum mean square estimate $\hat{\overline{z}}$ *of* $\overline{z}$ *given data* $\overline{\Lambda}$ *under these conditions is according to Gauss-Markoff theorem [11] equal to:*

$$\hat{\overline{z}} = \left(\overline{\overline{B}}^{T}\overline{\overline{B}}\right)^{-1}\overline{\overline{B}}^{T} \cdot \overline{\Lambda} \tag{4.8}$$

which reduces to (4.6) for a square matrix $\overline{\overline{B}}$*. The associated error matrix of the estimate is*

$$\overline{\overline{C}}_e = \left(\overline{\overline{B}}^{T}\overline{\overline{B}}\right)^{-1} \cdot \sigma_v^{\,2} \tag{4.9}$$

The numbers on the diagonal of this error matrix are the covariance coefficients of the fitted parameters, so the standard deviation of the fit is given by:

$$\sigma_z = \sqrt{\mathrm{trace}\left(\overline{\overline{B}}^{T}\overline{\overline{B}}\right)^{-1}} \cdot \sigma_v \tag{4.10}$$

where the trace function is the summing of the elements on the diagonal of a matrix.

Applying this theory to equation (4.5), the method becomes:

- Calculate the matrix $\overline{\overline{B}}$ with the elements:

  $$\overline{\overline{B}}_{n,i} = \sum_{j=0}^{J} k_{i,j}\left(T_n - T_0\right)^j$$

  with T_0 the reference temperature, T_n the temperature of measurement n, J the order of the polynomial fit and $k_{i,j}$ the polynomial fit coefficients for the temperature dependency of the mobilities;
- Create the conductivity vector $\overline{\Lambda}$, which is a column of N conductivity measurements at N different temperatures;
- Use equation (4.8) for finding the vector $\hat{\overline{z}}$, which is a column of the $z_i c_i l_i^0$ products of the I ions. Because z_i and l_i^0 are known, the concentrations of the individual ions can be calculated;
- The propagation of errors through this estimation method is represented by equation (4.10).

By examining equation (4.10) it can be seen that the accuracy of the estimation can be increased either by increasing the number of measurements or the temperature range.

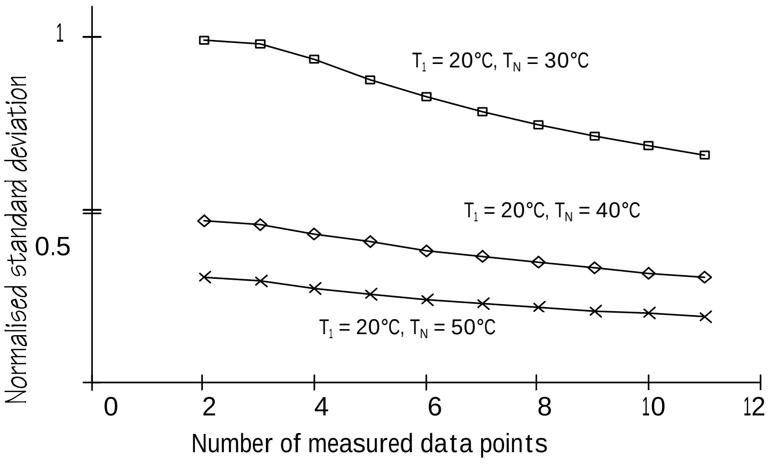

Figure 4.1: Effect of the temperature range and the number of measurements on the estimation accuracy.

Figure 4.1 shows that the improvement in accuracy by increasing the temperature range is larger than the improvement obtained by using more measurements.

4.3 A preliminary measurement

Using a Consort commercial conductivity measurement system, equation (4.8) was verified. The temperature compensation of the Consort was switched off, and the conductivity of a potassium chloride solution and a sodium chloride solution was measured at four temperatures between 21°C and 35°C. The result was fitted using the third order approximations of the temperature dependencies of the ions as given by Harned and Owen [10].

The potassium chloride solution was 10.8 mM and equation (4.8) showed $[K^+]$ = 14.5 mM and $[Cl^-]$ = 7.8 mM. The sodium chloride solution was 16.7 mM and the ion concentrations $[Na^+]$ = 16.9 mM and $[Cl^-]$ = 17.0 mM were found.

It is not very surprising that the fitting of sodium chloride is much more accurate then of potassium chloride because the mobility of potassium and chloride ions are almost equal which is not the case with sodium and chloride (a property used in chloride based reference electrodes).

Although the results are far from accurate, the method is still promising and will be evaluated in future. As was mentioned in section 2.4 the conductivity in tap water is determined for 90% by Ca^{2+}, Na^+, Cl^- and HCO_3^-. These ions can probably be measured using this method

5. Eliminating the reference electrode during amperometry

Of all measuring techniques mentioned here, only chrono amperometry for measuring hydrogen peroxide needs a (glass) reference electrode. However, according to the Cottrell equation (3.13), this absolute potential is actually not required for measuring. This gives rise to the idea that it can be substituted by a less good reference.

5.1 The reference with chrono amperometry

After a few milliseconds necessary for loading the electrical double layers, the measured current with chrono amperometry certainly is equal to the current passing the working electrode. With potentiometry, however, the measured potential contains an uncertain offset which comes from the electrode polarisation.

So the advantage of amperometry is that the absolute potential is not needed when the applied potential is in the good range. The condition for the applied potential is that it must be about 0.3V larger than the E^0 potential for the evoked reaction in order to deplete the surface immediately. Under this condition the measured current is independent on the applied potential. This independence can be used to check whether the experiment met the condition.

An option for measuring is the following. After doing a chrono amperometric experiment with $V_{appl} = E^0 + x$ and a second one with $V_{appl} = E^0 + y$, the measured current responses should be equal. However, the experiments must be performed in a period which is smaller than the variation time in the potential across the bad reference electrode.

5.2 Amperomtry with an added AC signal

The actual idea of this method is to find a potential at which small variations in the input potential do not result in variations in the measured current. So when using a ramp potential with a superponed AC signal, the output signal is “valid” when no AC current is being measured.

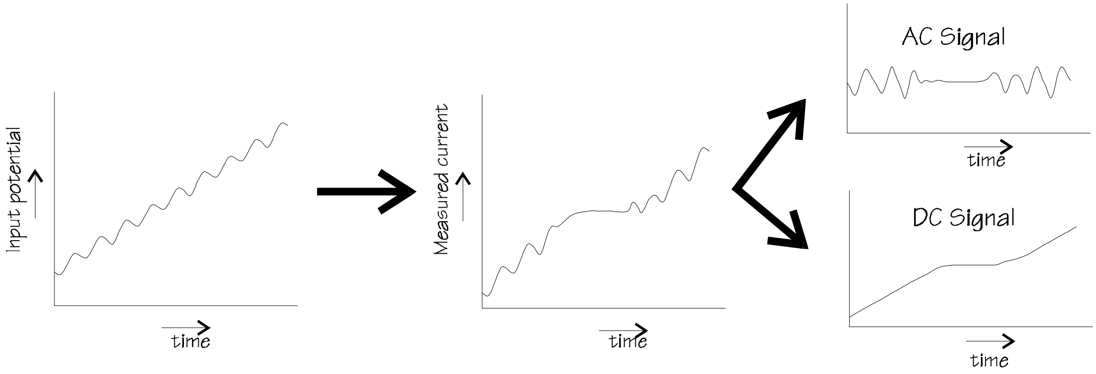

Figure 5.1: Finding the input potential independent area

Because the input signal is a ramp and not a step, the theory for the chrono amperometric experiment is not valid anymore. At 25 °C the peak current for potential sweep amperometry is equal to [12]:

$$i_p = \left(2.69 \cdot 10^5\right) n^{\frac{3}{2}} A D_0^{\frac{1}{2}} v^{\frac{1}{2}} C_0^{*} \tag{5.1}$$

with

n the number of electrons transferred,
A the size of the electrode [cm^2],
D_0 the diffusion coefficient of H_2O_2 [cm^2/sec],
v the scan rate [V/sec],
C_0^* the bulk concentration of H_2O_2 [mol/cm^3]
and i_p in amperes.

So in comparison to the Cottrell equation (3.13), all the parameters are equal except for the time which is now substituted by the scan rate v.

6. A stimulus-response measurement

In order to find new parameters, the operational points of the sensors should be controlled. The method described here uses the bad solubility of calcium ions in an environment with a high pH. When the pH in a sample is risen, for example by the electrochemical reduction of water, calciumhydroxide will deposit on the electrode. This thin layer of dielectric material can be measured by an impedance measurement using a conductivity cell.

6.1 Precipitation of $CaOH_2$ on a conductivity cell

The model developed here, assumes that no large error is being introduced when first the excess OH^--ion concentration profile is calculated, and afterwards is being decided how much Ca^{2+}-ions will precipitate. Actually, the precipitation reaction and the diffusion are coupled processes.

First, the diffusion of electrochemically generated OH^--ions from the working electrode into the sample is described. The chemical reaction of interest is:

$$2H_2O + 2e^- \rightarrow H_2 + 2OH^- \qquad (6.1)$$

so for each electron passing the electrode\electrolyte interface, one OH^--ion is being generated.
The diffusion of an instantaneously generated amount of OH^--ions by an infinitely large flat actuator is given by [13]:

$$c_{OH^-}(z,t) = \frac{e^{-\frac{z^2}{4D_{OH^-}t}}}{2\sqrt{\pi D_{OH^-}t}} \qquad (6.2)$$

with D_{OH^-} the diffusion coefficient and z the distance to the actuator. The response due to a constant electrical current i can be found from convolution in time:

$$c_{OH^-}(z,t) = \frac{i}{2FA\sqrt{\pi D_{OH^-}}}\left[2\sqrt{t}e^{-\frac{z^2}{4D_{OH^-}t}} + z\sqrt{\frac{\pi}{D_{OH^-}}}\left(\mathrm{erf}\left(\frac{z}{\sqrt{4D_{OH^-}t}}\right)-1\right)\right] \qquad (6.3)$$

where A is the electrode surface and F the Faraday’s constant. Figure 6.1 shows the concentration profile of the excess OH^--ions.

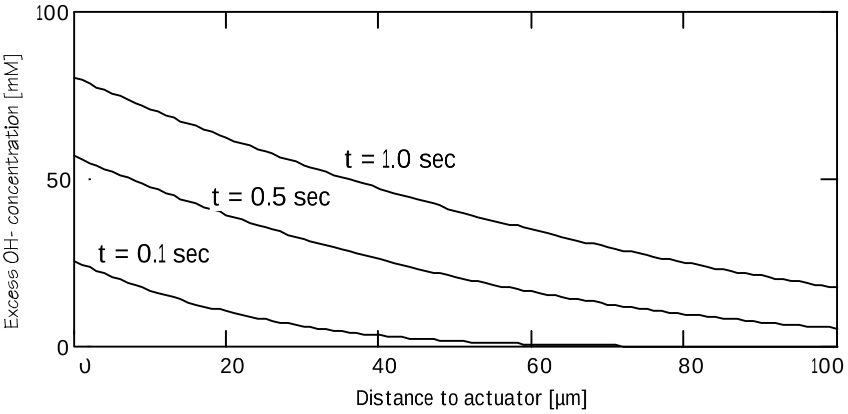

Figure 6.1: Excess OH$^-$ concentration profile

The next step is to find in which area calcium ions are able to precipitate. The equation for the solubility is:

$$k_s = [Ca^{2+}][OH^-]^2 \left(= 1.3 \cdot 10^{-6} \, mole^3 / l^3\right) \tag{6.4}$$

so when

$$[OH^-] > \sqrt{\frac{k_s}{[Ca^{2+}]}} \tag{6.5}$$

calcium is able to precipitate. If z_t is the thickness of the layer in which equation (6.5) is true, then the thickness d of the deposited $Ca(OH)_2$ film will be:

$$d = \frac{z_t \cdot m}{\rho}[Ca^{2+}] \tag{6.6}$$

with m the molar mass of $Ca(OH)_2$ (74.09 gram) and r the density of $Ca(OH)_2$ ($2.24 \cdot 10^3$ kg/m^3). Figure 6.2 shows a parametric plot of d versus [Ca^{2+}] using z_t as the independent parameter.

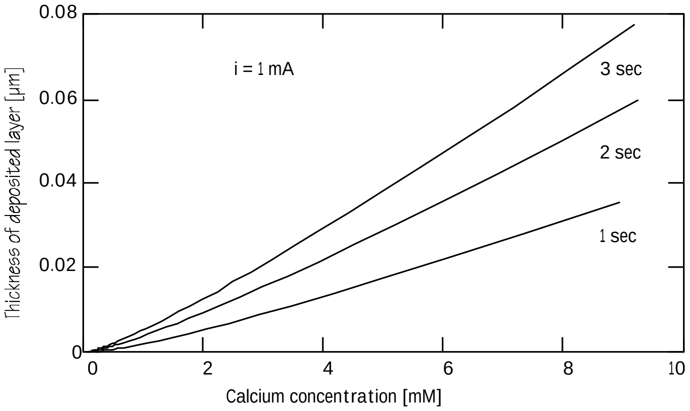

Figure 6.2: Thickness of the deposited $Ca(OH)_2$ layer

The interdigitated finger structure with a deposited $Ca(OH)_2$ layer is draw in Figure 6.3. The parameter of interest is $C_{Interface}$, the undesired component is R_{Sol}. When using the model of section 3.1 with the low cut-off frequency (3.8), it can be seen that the effect of the modulated $C_{Interface}$ is in this frequency.

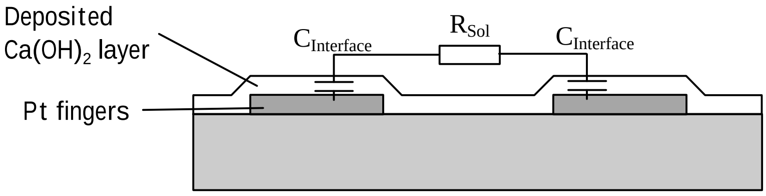

Figure 6.3: Schematic representation of the model

Unfortunately, the conductivity is unknown because an unknown amount of OH^- is being generated. Under certain circumstances however (for example when the background conductance is very high) this will not cause a large problem.

6.2 Lay-out of the devices

In principle the finger electrodes can be used to control the pH. However, for better performance some special devices were produced. The conductivity cells are identical to the ones of integrated sensor array type 1-3, but an extra actuator electrode was placed around them for a more homogenous pH distribution. These sensors are referred to as type I, II and III.

7. Conclusions

The integrated sensor array “array 1” includes the following basic structures:

- a working electrode;
- an interdigitated finger structure;
- a thermoresistive resistor.

Two versions were designed: an array version and an integrated structure version. If all the ideas work like expected, these basic structures can determine a lot of parameters:

- The temperature can be measured using the thermoresistive resistor;
- The interdigitated finger structure measures conductivity where the measured temperature can be used to compensate for example 2%/°C for the temperature dependency;
- Using the working electrode for chrono amperometry, hydrogen peroxide can be determined. The technique for determining the desired electrode potential for reduction of H_2O_2 at the electrode described in chapter 5 can be used to substitute the glass reference electrode by a relatively bad metal reference;
- By measuring conductivity at several temperatures (which can be done by heating using the thermoresistive resistor), the concentrations of ions can be fitted using polynomial approximations for the temperature dependencies of the separate ion conductivities. Because the conductivity in tap water is determined for 90% by Ca^{2+}, Na^{+}, Cl^{-} and HCO_3^{-}, this method might be an option for the measurement of water hardness;
- Another sensor/actuator approach for measuring water hardness is the precipitation impedance method. First calcium hydroxide is precipitated on a conductivity cell by locally increasing the pH (electrochemically generating hydroxyl ions by reducing water). The impedance measured by the conductivity cell is directly proportional to the thickness of the deposited layer and so to the calcium concentration.

So the measurements to be done are:

Device	Description	Measurements	Using
1, 2, 3	Integrated sensor arrays	- Resistivity vs. temperature	1, 2 or 3
		- Impedance vs. conductivity	1, 2 and 3
		- Chrono amperometry	1, 2 or 3
A, B	Multi purpose sensor structures	- Resistivity vs. temperature	A, B and C
		- Impedance vs. conductivity	A, B and C
		- Chrono amperometry	A, B and C
I, II, III	Conductivity sensors for $Ca(OH)_2$ deposition purposes	- Impedance before and after applied current in calcium solution	I, II and III
T1, T2, T3	Dual thermoresistive structures	- Temperature while heating with the other	T1, T2, T3

In the next work report these measurements will be reported. They will be performed using laboratory set-ups (potentiostat, gain/phase anayser). Afterwards the optimisation for the use in a simple on-line system can be done.

In future attention must be paid to the consequences of simultaneously measuring. This will involve both chemical and electrical interferences.

A. The silicon process

1. Wafer cleaning

Wafer:
Size: 3 inch
Thickness: 385 - 415 µm
Crystal: <100> p-type

Standard Wafer Cleaning:
5 min Fuming HNO_3 I
5 min Fuming HNO_3 II
Rinsing until conductivity < 0.1 µS
10 min hot HNO_3
Rinsing until conductivity < 0.1 µS

HF Dip:
A few seconds until hydrophobic

2. Wet thermal oxidation

Typical rate: 70 nm/min$^{1/2}$
Intended thickness: 1.5 µm
Using tube III:
Initially 800ºC (Setting 1)
484 min 1150ºC (Setting 8)
Cooling down to 800ºC (Setting 1)

3. Evaporation of Ta/Pt/Ta

Adheasion layer: 20 nm Ta
Pt Thickness: 250 nm
Adheasion layer: 20 nm Ta

4. Lithography using mask 1 "Conductors"

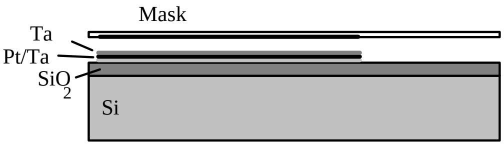

Resist:
spinning HMDS, 4000 rpm 20 sec
pos. resist (1813), 4000 rpm 20 sec
pre bake at 90 ºC during 20 min
exposure 8 sec mask 1
60 sec in 351 developer
post bake at 120 ºC during 30 min

Etching:
Ta: RIE
Pt: Pt-etchant ("Koningswater")
90 ºC ± 6 min
Ta: RIE

Stripping: Fuming HNO_3

5. Oxidation of Ta

1 hour 500 ºC in O_2

6. Polyimide

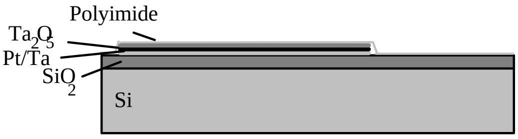

Dry surface in vacuum oven 150 ºC
Primer:
19 ml methanol
1 ml water
1 droplet APS (3-triethoxysilylpropylamin)
Polyimide:
PI : NMP (n-methylpyrolidon) = 5 : 1
Spinning of primer 4000 rpm 20 sec
Spinning of PI 4000 rpm 60 sec
Pre bake 90 ºC 25 min

7. Lithography using mask 2
"Contact holes and liquid-exposure areas"

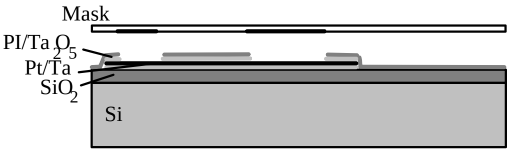

15 sec exposure using mask 2
Dry at 90 ºC during 10 min
Devel. polyimide in PI-developer during 2 min
Dry 30 min in vacuum oven 300 ºC
Remove Ta_2O_5 by RIE

8. Sawing, packaging and bonding

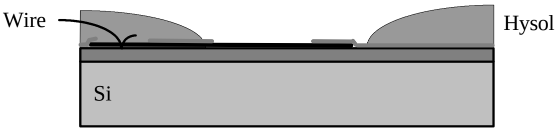

Material: Hysol

B. References

[1] Statistiek wateronderzoek 1986, Vereniging van exploitanten van waterleiding bedrijven in Nederland (VEWIN).

[2] P. Jacobs, A. Varlan, W. Sansen,
Design optimisation of planar electrolytic conductivity sensors, Medical & Biological Engineering & Computing, November 1995.

[3] E.A.M.F. Dahmen,
Electroanalysis, Theory and applications in aqueous and non-aqueous media and in automated chemical control, Elsevier, Amsterdam, 1986.

[4] M.R. Bekebrede,
Literatuurstudie naar: Electroden voor het detecteren van waterstofperoxide in de tuinbouw, Rapport Universiteit Twente, faculteit CT, juni 1996.

[5] R.S.C. Cobbold,
Transducers for biomedical measurements: principles and applications, John Wiley & sons, New York, 1974.

[6] R.G. Bankras, J.M. van der Neut, C.M. Lievers en E. Roos,
Integratie van meerdere sensoren op één chip, Verslag D1-project, BIO 96/14, Universiteit Twente 1996.

[7] D.M. Gray and A.C. Bevilacqua,
Unique temperature compensation for conductivity andresistivity measurements, Ultrapure water, volume 13, 1996.

[8] Toshiaki Isono,
Density, viscosity, and electrolytic conductivity of concentrated aqueous electrolyte solutions at several temperatures. Alkaline-earth chlorides, $LaCl_3$, Na_2SO_4, $NaNO_3$, NaBr, KNO_3, KBr and $Cd(NO_3)_2$. Journal of chemical and engineering data, Vol. 29, No.1, 1984.

[9] A.L. Horvath,
Handbook of aqueous electrolyte solutions, physical properties, estimation and correlation methods, Ellis Horwood Limited, Chichester,1985.

[10] H.S. Harned and B.B. Owen,
The physical chemistry of electrolytic solutions, Reinhold Publishing Corporation, New York, 1958.

[11] Paul B. Liebelt,
An introduction to optimal estimation, Addison-Wesley Publishing Company, Reading, Massachusetts, 1967.

[12] A.J. Bard and L.R. Faulkner,
Electrochemical methods, fundamentals and applications, John Wiley and Sons, New York 1980.

[13] H.S. Carslaw and J.C. Jeager,
Operational methods in applied methematics, Dover publications Inc. New York, 1947.

Distribution list:
P. Bergveld (UT BIO)
W. Olthuis (UT BIO)
A. Volanschi (UT BIO)
A.P.A.F. Rocourt (URL)